

Spectroscopy of 3D-trapped particles inside a hollow-core microstructured optical fiber

Charithra Rajapakse,¹ Fan Wang,² Tiffany C. Y. Tang,² Peter J. Reece,²
Sergio G. Leon-Saval,¹ and Alexander Argyros^{1,*}

¹*Institute of Photonics and Optical Science (IPOS), School of Physics, The University of Sydney, Australia*

²*School of Physics, The University of New South Wales, Sydney NSW 2052, Australia*

*alexander.argyros@sydney.edu.au

Abstract: We report on the demonstration of three-dimensional optical trapping inside the core of a hollow-core microstructured optical fiber specifically designed and fabricated for this purpose. Optical trapping was achieved by means of an external tweezers beam incident transversely on the fiber and focused through the fiber cladding. Trapping was achieved for a range of particle sizes from 1 to 5 μm , and manipulation of the particles in three-dimensions through the entire cross-section of the fiber core was demonstrated. Spectroscopy was also performed on single fluorescent particles, with the fluorescence captured and guided in the fiber core. Video tracking methods allowed the optical traps to be characterized and photobleaching of single particles was also observed and characterized.

©2012 Optical Society of America

OCIS codes: (060.4005) Microstructured fibers; (060.2280) Fiber design and fabrication; (350.4855) Optical tweezers or optical manipulation.

References and links

1. M. P. MacDonald, G. C. Spalding, and K. Dholakia, "Microfluidic sorting in an optical lattice," *Nature* **426**(6965), 421–424 (2003).
2. K. Dholakia, P. Reece, and M. Gu, "Optical micromanipulation," *Chem. Soc. Rev.* **37**(1), 42–55 (2007).
3. S. J. Hart and A. V. Terry, "Refractive-index-driven separation of colloidal polymer particles using optical chromatography," *Appl. Phys. Lett.* **83**(25), 5316–5318 (2003).
4. S. J. Cran-McGreehin, K. Dholakia, and T. F. Krauss, "Monolithic integration of microfluidic channels and semiconductor lasers," *Opt. Express* **14**(17), 7723–7729 (2006).
5. A. Yao, M. Tassieri, M. Padgett, and J. Cooper, "Microrheology with optical tweezers," *Lab Chip* **9**(17), 2568–2575 (2009).
6. P. S. J. Russell, "Photonic crystal fibers," *J. Lightwave Technol.* **24**(12), 4729–4749 (2006).
7. D. M. Gherardi, A. E. Carruthers, T. Cizmar, E. M. Wright, and K. Dholakia, "A dual beam photonic crystal fiber trap for microscopic particles," *Appl. Phys. Lett.* **93**(4), 041110 (2008).
8. F. Benabid, J. Knight, and P. Russell, "Particle levitation and guidance in hollow-core photonic crystal fiber," *Opt. Express* **10**(21), 1195–1203 (2002).
9. T. Takekoshi and R. J. Knize, "Optical guiding of atoms through a hollow-core photonic band-gap fiber," *Phys. Rev. Lett.* **98**(21), 210404 (2007).
10. P. Domachuk, N. Wolchover, M. Cronin-Golomb, and F. G. Omenetto, "Effect of hollow-core photonic crystal fiber microstructure on transverse optical trapping," *Appl. Phys. Lett.* **94**(14), 141101 (2009).
11. T. G. Euser, M. K. Garbos, J. S. Y. Chen, and P. S. J. Russell, "Precise balancing of viscous and radiation forces on a particle in liquid-filled photonic bandgap fiber," *Opt. Lett.* **34**(23), 3674–3676 (2009).
12. F. Benabid, J. C. Knight, G. Antonopoulos, and P. S. J. Russell, "Stimulated Raman scattering in hydrogen-filled hollow-core photonic crystal fiber," *Science* **298**(5592), 399–402 (2002).
13. F. M. Cox, A. Argyros, and M. C. J. Large, "Liquid-filled hollow core microstructured polymer optical fiber," *Opt. Express* **14**(9), 4135–4140 (2006).
14. F. M. Cox, A. Argyros, M. C. J. Large, and S. Kalluri, "Surface enhanced Raman scattering in a hollow core microstructured optical fiber," *Opt. Express* **15**(21), 13675–13681 (2007).
15. A. Argyros, M. A. van Eijkelenborg, M. C. J. Large, and I. M. Bassett, "Hollow-core microstructured polymer optical fiber," *Opt. Lett.* **31**(2), 172–174 (2006).
16. A. Argyros, "Microstructured polymer optical fibers," *J. Lightwave Technol.* **27**(11), 1571–1579 (2009).
17. M. A. van Eijkelenborg, A. Argyros, and S. G. Leon-Saval, "Polycarbonate hollow-core microstructured optical fiber," *Opt. Lett.* **33**(21), 2446–2448 (2008).

18. A. Argyros and J. Pla, "Hollow-core polymer fibers with a kagome lattice: potential for transmission in the infrared," *Opt. Express* **15**(12), 7713–7719 (2007).
 19. T. Birks, D. Bird, T. Hedley, J. Pottage, and P. Russell, "Scaling laws and vector effects in bandgap-guiding fibers," *Opt. Express* **12**(1), 69–74 (2004).
 20. G. J. Pearce, G. S. Wiederhecker, C. G. Poulton, S. Burger, and P. St. J. Russell, "Models for guidance in kagome-structured hollow-core photonic crystal fibers," *Opt. Express* **15**(20), 12680–12685 (2007).
 21. A. Argyros, S. G. Leon-Saval, J. Pla, and A. Docherty, "Antiresonant reflection and inhibited coupling in hollow-core square lattice optical fibers," *Opt. Express* **16**(8), 5642–5648 (2008).
-

1. Introduction

Micromanipulation using optical tweezers in a microfluidic environment has enabled a diverse range of capabilities to be explored. For example, the sorting of microscopic particles using microfluidic flow through an optical lattice has demonstrated the feasibility of optical fractionation based on the size, shape and refractive index of microparticles [1,2]. Other demonstrations include optical chromatography, in which optical and hydrodynamic forces are balanced to achieve segregation and collection of microscopic objects [3]. Microfluidic flow has been used to assist in loading static optical trapping geometries such as counter-propagating optical fiber traps and integrated laser traps [4]. Optical tweezers can generate microfluidic flow and can also be used for micro-rheology to map complex flow profiles [5].

Combining optical micromanipulation with microstructured optical fibers, also known as photonic crystal fibers [6], has also received growing interest. Special optical modes supported may be exploited for advanced trapping configurations, such as long range dual beam trapping using endlessly single-moded photonic crystal fiber (PCF) [7]. More attention has been received by hollow-core PCF (HC-PCF) and the possibility of trapping and guiding particles inside the hollow core. For example, the guided mode of the HC-PCF has been used to trap and guide Rubidium atoms and also particles along the length of a fiber [8,9]. The use of a tweezers beam focused transversely through the cladding of a water-filled fiber to load and hold a particle in the core [10] has been demonstrated using particles of approximately the same size as the core. Such particles would have filled the cross-section of the core and manipulation of their position would only have been possible along one dimension – longitudinally along the fiber. Recent studies have also shown liquid-filled HC-PCF can be used to probe viscous and optical forces on microparticles [11].

This combination of optical traps and HC fibers brings the possibility of interaction with the trapped particle using the optical waveguide (the hollow-core) in which the particle is trapped, beyond using the guided mode to perform the trapping. The HC fiber allows light to interact strongly with material filling the core, and this has been used, e.g., to generate frequency combs from Raman scattering in gases [12] in a silica HC fiber, or to characterize the optical rotation of a sugar solution [13] and to perform Raman spectroscopy [14] using HC microstructured polymer optical fibers (mPOF) [15,16]. In the latter example, a HC-mPOF filled with a Rhodamine/silver nanoparticle suspension was used to demonstrate improvements in the detection limit of surface enhanced resonant Raman scattering (SERRS). The improvement arose from guiding both the pump and SERRS wavelengths in the hollow core, increasing both the interaction with the pump light and the efficiency with which the SERRS signal was collected, relative to an equivalent measurement in a cuvette [14].

This paper reports on the first demonstration of three-dimensional optical trapping of microparticles inside the core of a liquid-filled hollow-core fiber, through the use of a conventional optical trapping configuration, i.e. an external tweezers beam focused transversely through the fiber cladding. Polystyrene spheres of 1-5 μm diameter were trapped and positioned throughout the cross section of the 60 μm diameter core of a HC-mPOF designed and fabricated for this purpose. The optical traps were characterized over the cross-section of the core using video tracking methods to determine the influence of the surrounding structure. Furthermore, this trapping architecture allows the HC fiber to be simultaneously

utilized as a waveguide, allowing spectroscopy on individual trapped particles to be conducted and photobleaching of individual particles to be observed.

2. Fiber design and fabrication

The requirements of this work necessarily place constraints on the properties of the hollow-core optical fiber. The fiber was required to have a large core to allow for a sufficient volume in which 3D trapping could be demonstrated but also a small external diameter ($< 200 \mu\text{m}$) to allow for positioning of the trapped particles throughout the transverse plane without the lens of the optical tweezers colliding with the fiber. The cladding was required to be as simple as possible to minimize distortions to the tweezers beam focused through it. To facilitate spectroscopy, the fiber would be required to have an appropriate transmission window, once filled with water, overlapping with the emission of the chosen fluorescent particles (550 to 700 nm in this case, as outlined in Section 4 below).

A polycarbonate (PC) kagome fiber with two rings of cladding holes [17] was chosen to address these constraints. Kagome fibers typically have a large pitch and a large core, and can achieve sufficient guidance without requiring many periods in the cladding [12,18]. Two rings of cladding holes minimizes both the complexity of the structure through which the tweezers beam is focused, and the diameter of the fiber. The wide transmission windows achieved in kagome fibers would also make it easier to accommodate the fluorescence spectrum of the particles. Polycarbonate is more rigid than the more commonly used polymethylmethacrylate (PMMA) [16] and would make the thin fibers easier to handle. The increased material absorption compared to PMMA would be negligible given the hollow core.

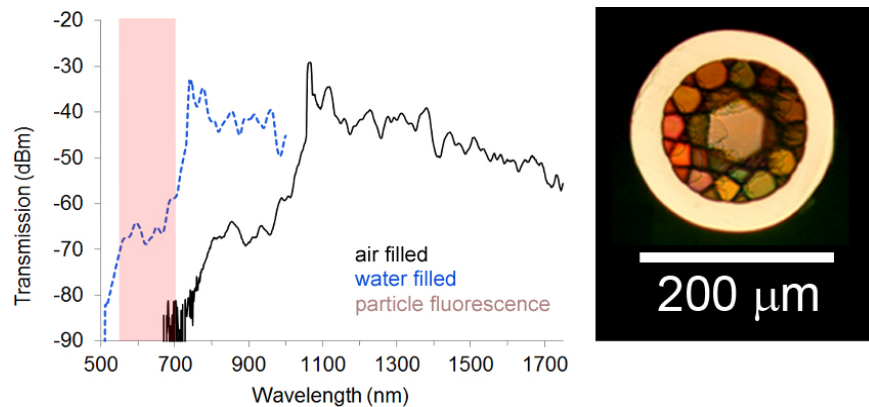


Fig. 1. Transmission spectrum (air-filled) of a 20 cm length of the fabricated fiber. The spectrum will shift upon water-filling to shorter wavelengths as show. The fluorescence range of the particles used in Section 4 is also indicated. Inset shows an optical microscope image of the end-face of the fiber used. This fiber is referred to as Fiber 1 in the text.

For ease of fabrication and handling, the fiber diameter must be maximized (i.e. to $200 \mu\text{m}$ in this case), requiring the blue edge of the transmission window to overlap with the particle fluorescence when filled with water. Considering the refractive index of PC ($n = 1.58$), filling with water shifts the wavelengths of the transmission windows to 70% of their value when filled with air [14,19], shown in Fig. 1. This required the air-filled fiber to guide wavelengths above approximately 800 nm, such that wavelengths above 550 nm may be guided when water-filled. This requires the polymer struts in the cladding of the fiber to have a thickness of approximately 320 nm [20,21].

The fiber preform was constructed by stacking 18 PC tubes with 4 mm diameter and $100 \mu\text{m}$ wall thickness inside a larger tube with 22 mm inner diameter/25 mm outer diameter. Two additional short tubes were inserted in the center of the stack at the top and bottom of the

preform to keep the central position (i.e. the core) open. The preform was stretched to cane of 8 mm diameter, from which fiber of 200 μm was drawn.

The cross-section of the fiber and the transmission spectrum (air-filled, 20 cm length) are shown in Fig. 1, with the main transmission band beginning at 730 nm and extending beyond 1750 nm. This will shift to a blue edge at 510 nm in the water-filled case, and hence will overlap with the fluorescence of the particles as required (Section 4), also shown in Fig. 1. The core diameter of the final fiber was approximately 60 μm , and the strut thickness was inferred from the transmission spectrum to be approximately 300 nm. The air fraction of the cladding was estimated to exceed 95%, and indeed the air fraction of the entire fiber exceeded 55%. This fiber will be referred to as Fiber 1 for the remainder of the paper.

In addition to the above fiber, a second kagome fiber as reported in [17] with the same geometry as Fiber 1, but slightly different dimensions, was also used. The transmission band of this fiber did not correspond to the wavelength region of interest here, and hence it was used for certain trapping experiments only, and not the characterisation of fluorescence in Section 4. This fiber will be referred to as Fiber 2.

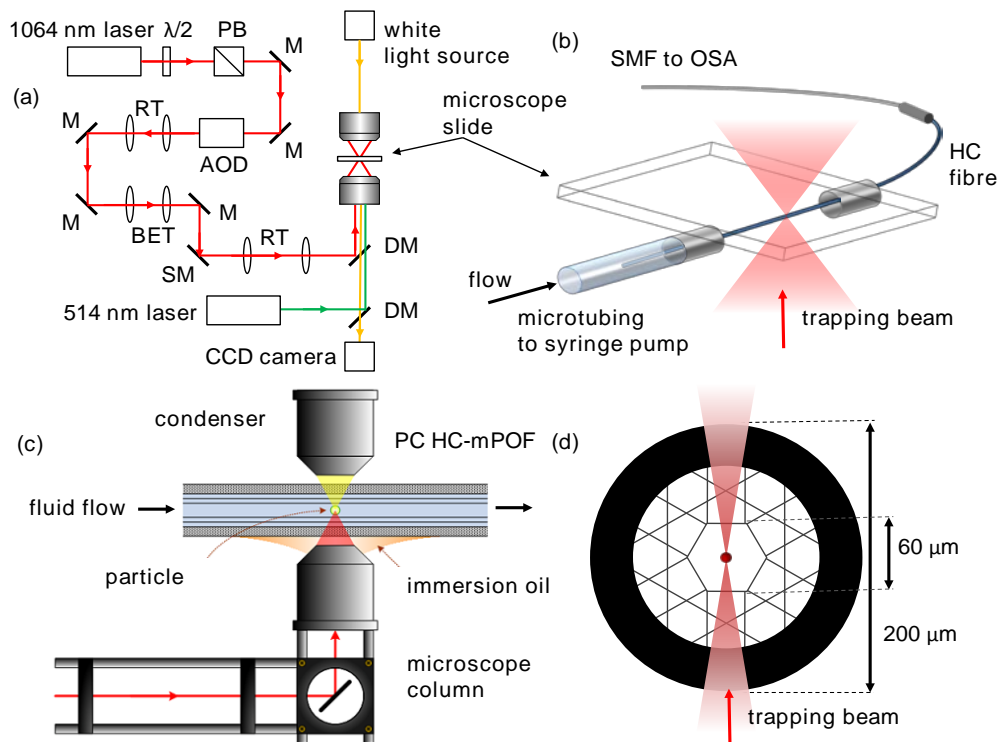


Fig. 2. (a) Schematic of the optical trap setup, with $\lambda/2$ indicating a half wave plate; PB a polarizing beam splitter; M a mirror; AOD the acousto-optic deflectors; RT a relay telescope; BET a beam expanding telescope; SM a steering mirror; DM a dichroic mirror. (b) Schematic of the microchamber constructed, with detail shown in (c). (d) Schematic of the HC fiber used for the trapping, showing the preferred orientation of the fiber with respect to the trapping beam; the dimensions indicated refer to Fiber 1.

3. Optical trapping inside the hollow-core

Details of the optical trapping setup used for this work are shown in Fig. 2. To facilitate trapping inside the fiber, a microchamber consisting of 10 cm of fiber was assembled as shown in Fig. 2(b). Two syringe needles cut to several mm's in length were glued to the edges of a microscope slide and the HC fiber was threaded through these and glued into place. Prior to gluing, the fiber's orientation was adjusted to minimize the number of interfaces the

tweezers beam would encounter as it passed through the cladding so as to minimize any possible distortions to the beam. The preferred orientation is shown in Fig. 2(d) and was discovered by trial and error throughout the course of the experiments.

Microtubing was attached to one of the syringe needles to allow the fiber to be filled with the suspension of the particles. The fiber protruding from the other needle was connected to a patch cord using SMA connectors, leading to an optical spectrum analyser (OSA). The patch cord was required to protect the OSA from the liquid exiting the fiber endface. After flushing with water, a suspension of the particles was introduced into the fiber through the microtubing. The flow speed was reduced to allow for the particles to be trapped.

The trapping experiments were conducted using a custom made optical tweezers apparatus, shown in Figs. 2(a) and 2(c). It consisted of a 5 W Nd:YAG (Laser Quantum Ventus) 1064 nm trapping laser, focused through a high numerical aperture (NA = 1.25) oil immersion objective to create a diffraction limited spot in the microscope imaging plane. A beam expansion telescope was used to overfill the back-aperture of the objective, and beam steering optics were used to translate the trapping beam using two-axis acousto-optic deflectors (AOD) or manually using a steering mirror. Bright field imaging was acquired through a camera. Variations in the particle position were extracted from video recordings of trapped particles.

Using this system, 1 μm and 5 μm polystyrene spheres were successfully trapped in the core (and also the cladding holes) of the HC fibers, using Fiber 1 and both fibers respectively. Figure 3 shows still frames from video footage of a 5 μm microsphere trapped in the center of the fluid-filled fiber (Fiber 2). In Figs. 3(a) and 3(b), trapping in the xy plane is shown by moving the trap position from side to side using the steering mirror, or by moving the fiber with respect to the static trap position. Three-dimensional trapping, shown in Fig. 3(c), is demonstrated by moving the trapping plane through different depths in the fiber via the sample stage and noting that the trapped particle remains in focus, with different layers of the surrounding microstructure becoming visible as depth changes (highlighted in red). These results demonstrate full three dimensional control of microscale objects inside an optical fiber, with position capabilities over a large volume inside the hollow core at accuracies comparable to gradient force optical tweezers. Videos of 5 μm and 1 μm particles being manipulated are shown in Fig. 4. The trapping powers used were 17 mW for the 5 μm particles (Fiber 2) and 40 mW for the 1 μm particles (Fiber 1). It is noted that in each instance of trapping across all the experiments, the particle was trapped using low laser power, and the power was increased to the desired value with the trapped particle remaining in focus. This confirms once again that 3D optical trapping was achieved, and not levitation of the particles in the z -direction.

An optical trap can be described as a microscopic Hookean spring with a restoring force F given by $F = -\kappa\Delta x$, proportional to the displacement Δx about the center of the trap and the trap stiffness κ . The trap stiffness was determined by analyzing video recordings of trapped particles to determine the positional variations, which were then decomposed in to variations in the x and y directions. A Gaussian distribution was fitted to the position data, allowing the variance σ of the best fit to be extracted, and the trap stiffness to be calculated from $\frac{1}{2} k_B T = \frac{1}{2} \kappa \sigma^2$, where k_B is the Boltzmann constant and T the ambient temperature. Examples of the position distributions and associated Gaussian fit for 5 μm particles trapped in the center of the core using a 20 mW trapping beam and Fiber 2 are shown in Fig. 5(a). This method does not allow for trap stiffness in the z -direction to be measured as fluctuations in position along z cannot be accurately discerned in the video.

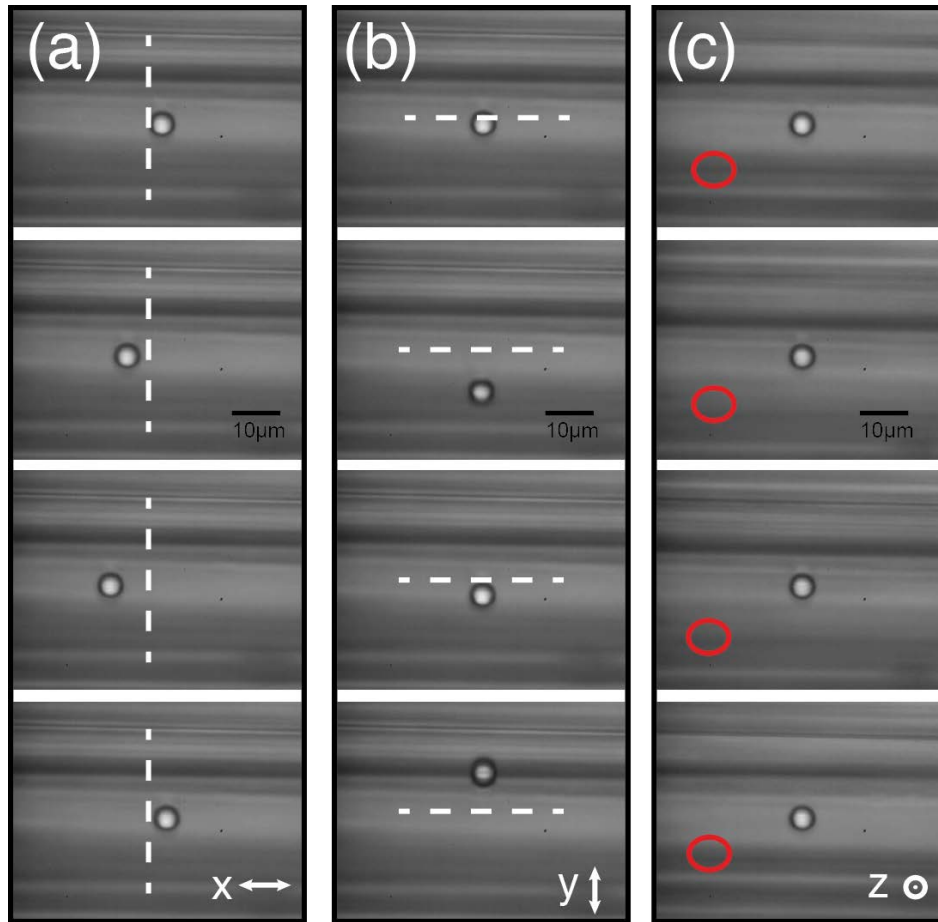


Fig. 3. Video frames showing the 5 μm particles trapped in the core of the HC fiber (Fiber 2). (a) Movement in x -direction along the direction of flow. (b) Movement in the y -direction across the transverse direction of the fiber. (c) Movement in the z -direction from the upper to the lower edge of the core with reference points highlighted in red. The laser power used was 16 mW.

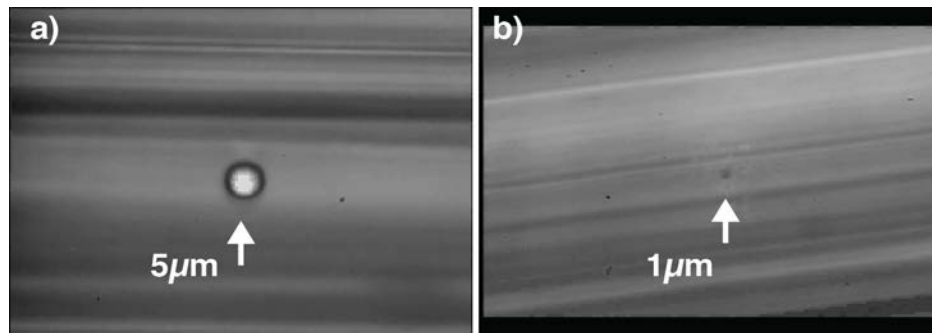


Fig. 4. Manipulation of trapped (a) 5 μm and (b) 1 μm particles in 3D inside the HC Fibers 2 and 1 respectively (see [Media 1](#) and [Media 2](#)).

Trap stiffness measurements were performed on the trapped 5 μm particles in Fiber 2 at different points along the core (at a constant trapping depth of 10 μm above the cladding holes) in order to assess the effect of the near-lying microstructure on the trapping performance. The particle was trapped at a power low enough to observe thermal fluctuations

within the trap. The particle position fluctuations such as shown in Fig. 5(a) allowed the trap stiffness to be calculated, and the variation in the trap stiffness across the core of the fiber is presented in Fig. 5(b) for both the x -direction (κ_x) and y -direction (κ_y). Points were taken where the image of the trapped sphere was suitably undistorted to allow video tracking with high fidelity. Important features to note about the trapping profile are that at the periphery of the fiber core the trapping stiffness is lower and more symmetric than the trap at the core center. Near the center of the core the trap stiffness is slightly higher along the direction of the fiber and at points where the trapping beam passes through struts in the cladding the trap stiffness becomes asymmetric.

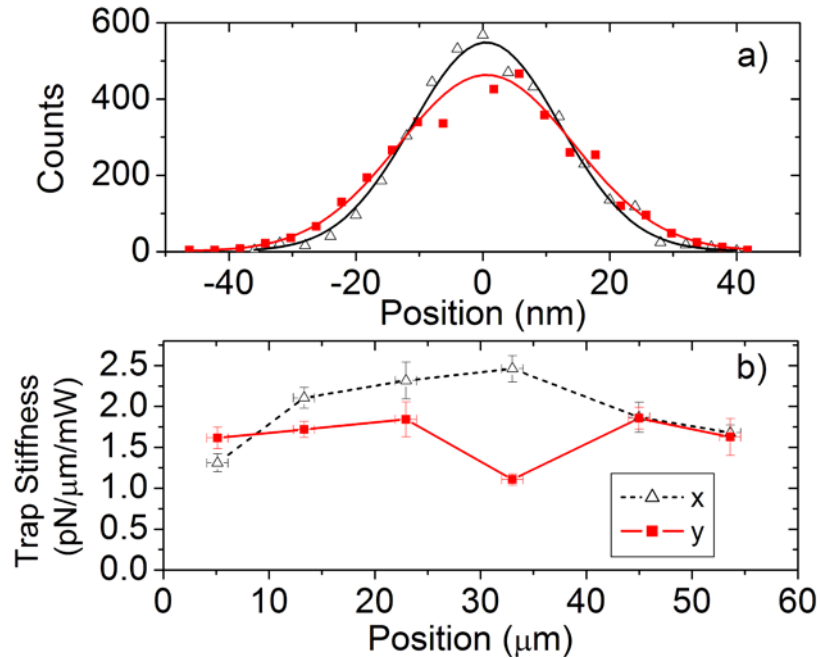


Fig. 5. (a) Histogram (symbols) and corresponding Gaussian fit (line) of position fluctuation of the microparticles trapped in the fiber core for the x - and y -directions, as measured using video tracking, with $5\ \mu\text{m}$ particles in Fiber 2. A Gaussian fit is used to determine the trap stiffness in each direction. (b) Profile of the variation in trap stiffness at different points along the width of the fiber core.

Qualitatively we can rationalize all of the important features shown in Fig. 5(b). At the edge of the core the trapping beam passes through a greater thickness of high refractive index polycarbonate, both in the coating and cladding layers, which leads to greater levels of spherical aberrations at the trapping site, thereby lowering the trapping strength. At the center of the fiber the strong asymmetry in the trap stiffness emerges due to an increase in diffraction from the underlying cladding structure along the width of the fiber. This is supported by the strong dip in trap stiffness when the trapped object passes near a cladding strut with a thickness of the order of the trapping wavelength. In the direction along the axis of the fiber the microstructure has extended features, which will perturb the trapping potential to a lesser extent.

4. Characterisation of trapped particles

Successfully trapping the particles inside the hollow-core of the fiber places these trapped particles inside a waveguide, meaning the guided modes of the waveguide are available to characterize the particles. The example application investigated in this work was to use $3.2\ \mu\text{m}$ diameter fluorescent particles (Thermo Fisher Scientific, Fluoro-Max Red R0300) and to

use the hollow-core to guide the fluorescence to an OSA (Fig. 2(b)). The particles obtained had an emission spectrum spanning from 550 to 700 nm (Fig. 6), and could be excited using a 514 nm argon-ion laser focused on the trapped particles through the same objective as the trapping beam (see Fig. 2(a)). Fiber 1 was used exclusively in this section.

Figure 6(a) shows the fluorescence spectra recorded through the hollow-core for a single trapped particle using 10 mW of power at the excitation wavelength. A fluorescence signal was only detected at the output of the fiber when a particle was held in the trap, and disappeared when the particle was released, confirming that the recorded fluorescence was of the single trapped particle. A comparison to the emission spectrum of a suspension of the particles, taken in a separate cuvette measurement, shows that the full spectrum was guided by the hollow-core as intended. Modulations in the spectrum collected via the fiber, as compared with the free particle cuvette measurement, are associated with the fiber's transmission properties. The intensity of the emission was observed to decrease with time, both through the spectra and through imaging (Fig. 6(b)). This indicates that the particles are photobleached by the excitation beam. The rate of photobleaching was estimated from the spectra of Fig. 6(a), and the emitted power was found to have a half-life of 16 s in the case of 10 mW excitation power. Particles that had been previously trapped could be identified when trapped subsequently through the lack of fluorescence, having been bleached.

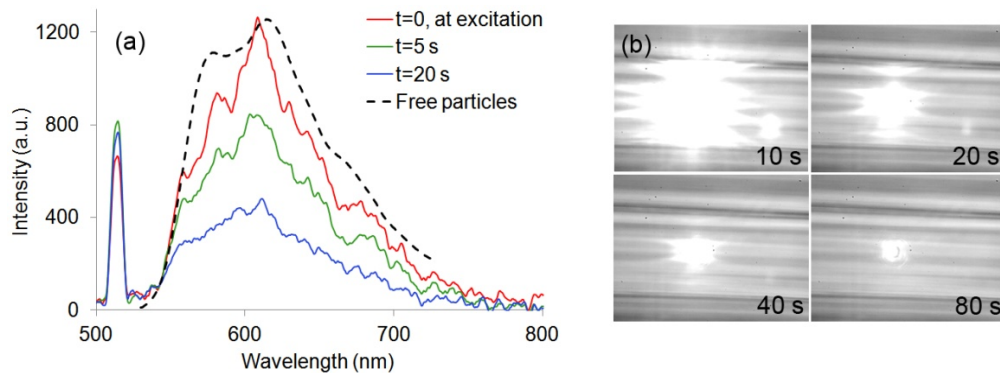


Fig. 6. (a) Emission spectra taken for different excitation times (514 nm, 10 mW) of a single trapped particle; the emitted light is guided through the hollow core of the fiber in which the particle was trapped. The spectrum of free particles in suspension is superimposed for comparison. The emission is observed to decrease with exposure to the excitation beam, in the spectra and also through imaging (b), indicating photobleaching. The peak at 514 nm is light from the excitation laser scattered into the core by the particle.

5. Conclusion

In conclusion, a novel trapping geometry has been demonstrated where a single gradient force optical tweezers was used to manipulate microscopic particles in three dimensions inside a hollow core microstructured optical fiber. Trap stiffness measurements were made using video tracking methods in order to determine the effect of the cladding structure on the trapping performance of the optical tweezers. Furthermore, light emission from an optically trapped fluorescently labeled microparticle was measured via a spectrometer coupled to the end of the hollow-core fiber. Particles were excited via a secondary laser source aligned co-linearly with the trapping laser. Measurements of photobleaching of the luminescence using the spectrometer and by directly visualizing the particle at the same time, as well as the absence of a fluorescence signal when no particles were trapped, confirmed that the signal was only originating from the trapped particle.

This work can be extended to the trapping of single cells suspended in solutions, and the characterisation thereof using fluorescence as demonstrated here, or other spectroscopy methods. Such a scheme would be identical to that presented, however cells would be

typically larger ($>10\ \mu\text{m}$) and will have a lower refractive index than the particles used here, closer to the refractive index of water. The resulting lower refractive index difference will reduce the optical forces, however, trapping in the geometric optics limit is less sensitive to aberrations, and this would improve the trapping capabilities inside the fiber. The fiber, as a waveguide, can be used to supply the pump light (for fluorescence or Raman spectroscopy), or to guide a broad wavelength range for absorption spectroscopy.

Acknowledgments

S.G. Leon-Saval is supported by an Australian Research Council Australian Postdoctoral Fellowship. A. Argyros is supported by an Australian Research Council Australian Research Fellowship. This work was performed in part at the OptoFab node of the Australian National Fabrication Facility, a company established under the National Collaborative Research Infrastructure Strategy to provide nanofabrication and microfabrication facilities for Australian researchers.